Journal of Civil Engineering and Management
ISSN 1392-3730 / eISSN 1822-3605
2019 Volume 25 Issue 6: 495–517
https://doi.org/10.3846/jcem.2019.8002

DAMAGE DETECTION FOR UHPFRC COMMUNICATION TOWER BASED ON FREQUENCY DATA AND PARTICLE SWARM OPTIMIZATION

Sarah JABBAR[1], Farzad HEJAZI[1*], Ammar N. HANOON[2], Rizal S. M. RASHID[1]

[1]*Department of Civil Engineering, University Putra Malaysia, Malaysia*
[2]*Reconstruction and Projects Department, University of Baghdad, Baghdad, Iraq*

Received 22 March 2018; accepted 19 December 2018

Abstract. Advances in the telecommunication and broadcasting sectors have increased the need for networking equipment of communication towers. Slender structures, such as towers, are sensitive to dynamic loads, such as vibration forces. Therefore, the stability and reliability performance of towers can be maintained effectively through the prompt detection, localization, and quantification of structural damages by obtaining the dynamic frequency response of towers. However, frequency analysis for damaged structures requires long computational procedures and is difficult to perform because of the damages in real structures, particularly in towers. Therefore, this study proposed a correlation factor that can identify the relationship between frequenciesunderhealthy and damaged conditions of ultra high performance fiber-reinforced concrete (UHPFRC) communication towers using particle swarm optimization. The finite element method was implemented to simulate three UHPFRC communication towers, and an experimental test was conducted to validate and verify the developed correlation factor.

Keywords: communication towers, ultrahigh performance concrete (UHPC), dynamic nonlinear analysis, frequency response, correlation factor, finite element method, particle swarm optimization (PSO).

Introduction

Damages caused by various factors may occur in structures during their intended lifespan. These damages must be located and measured to ensure the safety of structures. Many researchers have proposed techniques for detecting structural damages based on different types of structural characteristics or responses. The natural frequencies of structures are the most appropriate response candidates for damage detection (Kaveh & Zolghadr, 2015).

Determining the change in natural frequency can be used as a damage detection approach in structural assessment. This method offers the advantages of fast and easy frequency measurements (Sinou, 2009). Several investigations have been conducted to identify structural damages by using natural frequency approaches. Yang, Swamidas, and Seshadri (2001) used frequency change against crack depth in 3D plots, including location, to detect a saw cut in a beam made of aluminum material. The result of the obtained frequency change contour lines were plotted and overlaid. The intersection points yielded the actual depth and location of the crack. Ren and De Roeck (2002) proposed a method for predicting the location and severity of a damage by using changes in frequencies, mode shapes, and finite element methods (FEMs). Their method, which was validated using simulated and real measurement data, yielded satisfactory results. Kim and Stubbs (2002) introduced an algorithm that uses only low modes of vibration to identify the location and intensity of structural damage. The algorithm was verified on a two-span continuous beam and achieved good accuracy in indicating the location and severity of damage. Kessler et al. (2002) investigated the influences of different types of damage (delamination, impact damage, drilled-through holes, bending-induced cracks, and fatigue damage) on frequency response by using clamped composite plates. The authors concluded that fatigue damage is the only distinguishable type of damage with in the low-frequency range. Smith and Shust (2004) studied bounding natural frequencies in structures wherein natural frequency is affected mainly by the given boundary conditions, cross section, material function sensitivity, and size function sensitivity. Sutar (2012) used Finite element method (FEM) on a cantilever beam under cracking and examined the relationship among the natural frequen-

*Corresponding author. E-mail: *farzad@fhejazi.com*

cies of a model with crack depth and location. The results showed that the natural frequency of the model decreases with an increase in crack depth and location from the fixed end. The dynamic analysis of tall slender structures is generally performed in the frequency domain based on the characteristic-dependent frequency of the mechanical properties and loads on the structure.

Towers are tall slender structures where radio transmitters and their accessories are installed. These structures house a considerable number of equipment that transmits electromagnetic waves and ensure the proper operation of various services, such as mobile communication, television, and radio. However, the structural system of towers is susceptible to damage due to the heavy wind effect. Thus, the material and geometric properties, boundary conditions, and system connectivity of these structures can affect system performance if they are not designed appropriately (Guidorzi, Diversi, Vincenzi, Mazzotti, & Simioli, 2014). Structural damages reduce stiffness, thereby decreasing the natural frequency of a system. Therefore, the dynamic response of a structure must be investigated, particularly when the first natural frequency of the structure is less than 1 Hz.

Negm and Maalawi (2000) proposed optimization models of a wind turbine tower. These models showed thatoptimizing the weighted sum of the natural frequencies of a system represents the objective function and ensures balanced improvement in stiffness and mass. Grünbaum (2008) calculated the frequencies of tall building structures and displacements using 3D FEM with three different structures and compared their behavior to wind load. The results showed that frequency increases with the stiffness of a building, where as it decreases as building weight increases. Antunes, Travanca, Varum, and André (2012) presented a dynamic monitoring system of two tall slender steel telecommunication towers with a height of 50 m located in Portugal by using the frequency domain. The results indicated that stiffness loss occurs due to the connections and degradation of existing materials. Saisi, Gentile, and Guidobaldi (2015) explored the dynamic monitoring system of the 54.0 m-tall Gabbia Tower in Mantua, Italy using damage identification based on shifts in natural frequencies. The effects of post-earthquake conditions and temperature on the frequency of the tower were also investigated. The results indicated increases in temperature and modal frequencies, whereas the natural frequency of the fundamental modes was reduced because of the far-field seismic activities. Moreover, the authors found that temperature variation has no considerable effect on the frequency of the tower.

Several investigative approaches have been used to identify damages in civil structures and to differentiate various types of damage. Diverse approaches have been undertaken. For example, some investigations focus on identifying damage locations, whereas others rely on monitoring damage initiation. The optimal solutions for any system can be defined as feasible solutions with an objective function value and any other feasible solutions attained through the selection of values for a set of parameters that satisfy all the constraint solutions (Rardin, 1998). Many parameters and variations affect the extent of damage and inter operation of accurate decision data on damage occurrence. In recent years, various optimization techniques have been implemented to enhance the accuracy of the damage detection and health monitoring systems of structures. Mhaske and Shelke (2000) detected the depth and location of a crack in a cantilevered beam using the vibration measurement test with the aid of an artificial neural network (ANN) and a genetic algorithm (GA). The authors found that GA is an accurate search method for obtaining the desired results in vibrating structures or beams. The validation of the experimental results with ANN showed an acceptable similarity. Paultre, Weber, Mousseau, and Proulx (2016) developed a sensitivity-based damage identification approach. The system works based on the model update applied to a full-scaletwo-story structure made with high-performance concrete (HPC) under earthquake excitations. The investigation was performed to obtain mode shapes, modal damping, and resonant frequencies. Dua, Watkins, Wunsch, Chandrashekhara, and Akhavan (2001) proposed a new classification approach for identifying damages caused by impact on composite plates using ANN and FEM. Compared with other soft computing tools, particle swarm optimization (PSO) is efficient and requires only a few function evaluations to yield the same quality or improve the results (Ashour & Rishi, 2000; Dong, Xu, & Lin, 2017; Alaghebandha, Hajipour, & Hemmati, 2017). Kazemi et al. (2011) proposed an ANN and a PSO based on certain procedures to determine the depth and location of cracks in cantilever beams. The first three natural frequencies of beams were obtained from FEA and applied as inputs for ANN. PSO was applied to train ANNs to predict the depth and location of cracks. The results are in good agreement with the actual data, thereby exhibiting the feasibility of using an ANN that is trained with only natural frequency data.

Begambre and Laier (2009) reported that improved results were obtained in identifying structural damage when data frequency and FE analyses were performed on a 10bar truss and crack-free beam, which effectively determined damage location using the PSO-simplex algorithm. As warm optimization algorithm has also been applied to detect structural damage in truss by observing changes in vibrations using ant colony optimization (Majumdar, Nanda, Maiti, & Maity, 2014), which exhibited varying levels of success in accurately determining structural damage from the results. Nhamage, Lopez, and Miguel (2016) proposed a hybrid stochastic/deterministic optimization algorithm for detecting damage in a cantilever beam due to changes in vibrational frequencies. They reported that the model performed efficiently in detecting damage from a cantilever beam.

The aforementioned literature review shows that natural frequencies are appropriate parameters for assessing the health condition of structures because frequencies depend on stiffness and indirectly reflect the stability and

strength of a structure. The dynamic frequency response of healthy and damaged structures can be used to identify any damage. However, accomplishing this task is difficult when numerical and experimental methods that require numerous calculations are used. Therefore, this study proposed a dynamic frequency correlation factor for identifying the relationship between frequenciesunderhealthy and damaged conditions for ultrahigh performance fiber-reinforced concrete (UHPFRC) communication towers using PSO.

1. Dynamic response of the structure

In the past, several on-model-based damage identification algorithms have been developed using different dynamic characteristics, such as modes, shapes, and natural frequencies. The change in natural frequency is associated with the degradation of a structure. Thus, this parameter can be an indicator of the stability of a structure and the preventive measures that can be taken to save cost and the lives of inhabitants. Frequency can be used to evaluate the dynamic performance of a structure because it affects the stability and strength of the structure.

The dynamic analysis of tall slender towers is commonly performed in the frequency area in consideration of the frequency-dependent and mechanical properties of a building. In accordance with the Eurocodes EN 1991-1-4 (CEN, 2005), EN 1993-3-1 (CEN, 2006), simplified quasi-static design procedures can be adopted with suitable gust response factors that depend on various parameters, such as damping factor, first natural frequency, and structural characteristic. In the design approach of the Eurocodes, the first natural frequency is a key parameter for estimating the response of a structure. The natural frequencies of towers, with variations in height and geometric characteristics, have been reported by different researchers.

The evaluation of frequency using numerical and experimental methods requires numerous calculations. Therefore, this study proposed a correlation factor for identifying the relationship between frequencies under healthy and damaged conditions of structures. The result can be used to identify cracks.

2. A correlation factor of damage frequency of UHFPRC communication tower

To identify the relationship between the frequencies under healthy and damaged conditions of UHPFRC communication towers, a correlation factor was used by applying PSO, as presented in Eqn (1):

$$f_{damage} = \text{correlation factor} \times f_{healthy}, \quad (1)$$

where: f_{damage} – damage frequency of the tower, $f_{healthy}$ – healthy frequency of the tower.

To formulate the damage frequency ratio (Eqn (1)), the frequency of the structure under healthy condition should be determined (through numerical simulation or experimental test). However, as mentioned earlier, temperature variation does not affect frequency response.

A new development was achieved with regard to the capability of the indicator as a correlation factor in detecting and relatively quantifying damages. Three key points must be considered in its development: (a) the objective function must be formulated, (b) a clear method for solving the optimization problem must be developed, and (c) the convergence criteria must be defined. These itemized points are discussed in the succeeding sections. A communication tower made of UHPFRC with a hollow circular section was considered. This tower consisted of three segments that were connected to one another using bolts and nuts at the joints.

3. Considered communication tower

The UHPFRC communication tower used in this study was based on an actual tower located in Malaysia with a height of 30 m. The tower model was composed of three segments, and each segmentwas10 m high, bolted together at joint locations, and fixed to a reinforced concrete foundation base with a length, width, and depth of 4×4×1 m (Figure 1).

Figure 1. UHFPRC communication tower located in Malaysia

A fixed connection was applied to provide sufficient lateral stiffness for the tower and to link the prestress reinforced concrete segmental sections to one another using bolts and nuts. The length and diameter of the bolt were 1000 mm and 25 mm, respectively, in the connection joint. Meanwhile, the bolts in the foundation connection were 1000 mm and 32 mm in length and diameter, respectively. Each segment was arranged in eight tendons, and each connection was arranged in eight holes for the bolts. The total mass density for the ultrahigh performance concrete was 2500 kg per m^3 using a grade of 150 MPa, a Young's

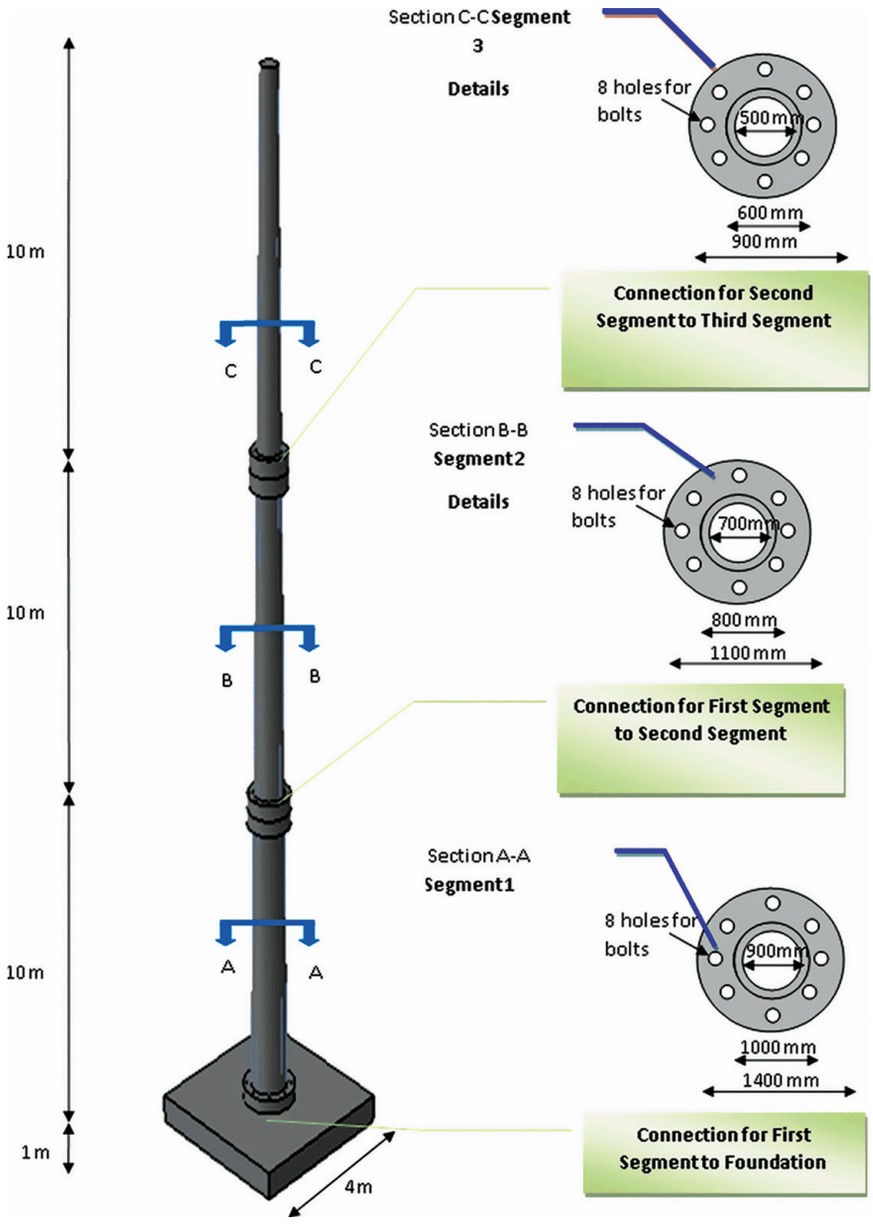

Figure 2. Developed FEM for typical UHPFRC communication tower (15 m, 30 m and 45 m height)

modulus of elasticity of 55 GPa, and a Poisson's ratio of 0.18. The segments were internally prestressed using tendons with a diameter of 15.2 mm and a Young's modulus of 200 GPa. Figure 2 shows the modeled tower.

FEM was used to develop three communication towers with heights of 15, 30, and 45 m to establish the frequency correlation factor. The tower with a height of 30 m was tested experimentally to verify the results and develop the PSO algorithm for damage correlation, whereas the towers with heights of 15 m and 45 m were used to validate the algorithm. Different damage scenarios were created using FEM. The damages involved individually removing one to six bolts from each connection for the full-scale tower. Then, 87 cracks, which consisted of vertical and horizontal cracks at every 1 m of the communication tower, were simulated.

4. Development of FEM

Numerical analysis was conducted to evaluate the modal parameters (particularly the natural frequencies) of the precast UHPFRC communication tower under various conditions. The performance of the communication tower was investigated under free vibration in healthy and different damage cases. A 3D nonlinear finite element program, ABAQUS (Dassault Systèmes Simulia Corp., 2014), was utilized to model the three UHPFRC communication towers with heights of 15 m, 30 m, and 45 m under healthy and damaged conditions, as shown in Figure 3. The 30 m tall tower was tested experimentally to verify the numerical results (Table A.2, Appendix) and develop the PSO algorithm for damage correlation, whereas the 15 m and 45 m tall towers were used to validate the algorithm. Then, 3D finite element software with an eight-node solid element was used

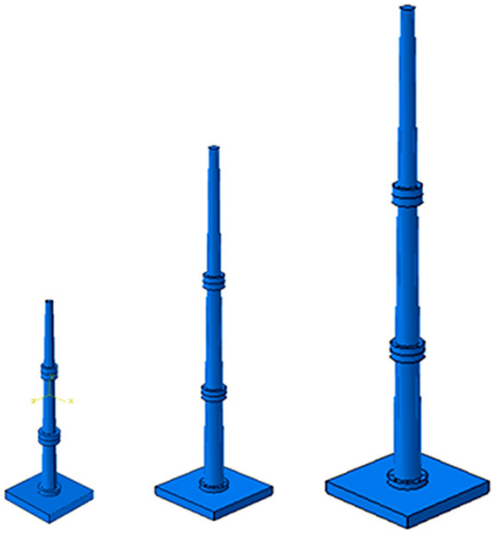

(a) 15 m height (a) 30 m height (a) 45 m height

Figure 3. Developed UHPFRC communication towers with 15 m, 30 m, and 45 m height

to simulate the three concrete UHPFRC communication towers with heights of 15 m, 30 m, and 45 m.

A two-node linear 3D truss element was used to model the reinforcing bar and pressurizing tendon elements that were embedded into the concrete. Screws and nuts were used to integrate the different parts of the proposed connection. For the segment connection, the screw and nut were created as solid parts with the bolts having a length and diameter of 1000 mm and 25 mm, respectively. The diameter of the bolts for the foundation and the first segment connection was 32 mm.

The structured and sweep technique was adopted for meshing. All the models meshed with a sieve of 150 mm are shown in Figure 4.

Figure 4. UHFPRC Tower Mesh (15 m, 30 m, and 45 m height)

Figure 5. Applying boundary condition for UHFPRC communication tower

A fixed boundary condition was applied to the UHPFRC communication tower foundation, as shown in Figure 5. The boundary condition is defined in Eqn (2):

$$U_1 = 0,\ U_2 = 0,\ U_3 = 0,\ UR_1 = 0,\ UR_2 = 0,\ UR_3 = 0, \quad (2)$$

where U is the translation, and UR is the rotation.

The Lanczos eigen solver analysis was implemented to generate frequency.

5. Frequency results of the 30 m UHPFRC tower

Numerical analysis was conducted to investigate the frequency response of the UHPFRC communication tower under healthy condition for the first 11 modes of vibration before damage, as listed in Table 1, for the first 11 modes of vibration before damage.

Figure 6 shows the mode shapes that correspond to the frequencies of the UHPFRC communication tower under healthy condition.

A full-scale UHPFRC communication tower in a healthy state was tested experimentally via an experimental modal analysis test using a Kistler impact hammer (model 9728A20000) to evaluate the frequency response and verify the numerical frequency responses of the tower, as shown in Figure 7. The signal was measured using three accelerometer sensors attached to the specimen to determine the first 11 natural frequencies.

Table 1. Verification result of the experimental and numerical tower

Mode No.	Mode 1	Mode 2	Mode 3	Mode 4	Mode 5	Mode 6	Mode 7	Mode 8	Mode 9	Mode 10	Mode 11
$f._{EXP}$	0.9	1.13	3.45	8.63	15.36	18.1	42.83	79.21	101.56	119.46	138.49
$f._{FE}$	0.93	0.94	3.8	8.87	17.79	20.1	41.35	74.15	104.14	113.86	137.44
$[(f._{EXP} - f._{FE}) / f._{EXP}]\%$	–0.03	0.19	–0.35	–0.24	–2.43	–2	1.48	5.06	–2.58	5.6	1.05

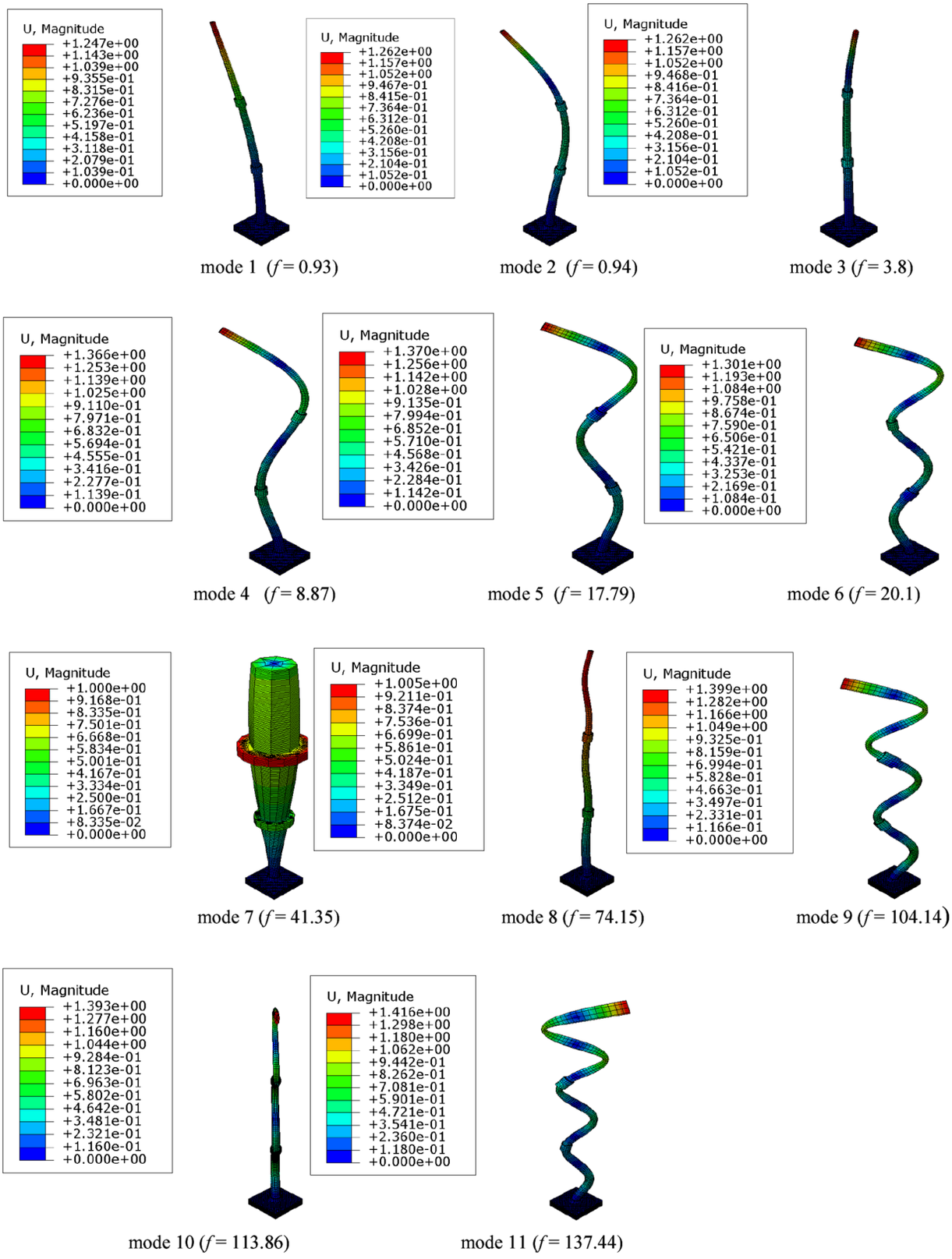

Figure 6. Mode shapes of the UHPFRC communication tower

Figure 7. Impact hammer

Figure 8. Accelerometer

The test procedures are described as follows.

1. Three Kistler accelerometers (model 8702B50M1) were used to record acceleration response, as shown in Figure 8. Each accelerometer was placed in a specific position.
2. The position of the knocking point was marked.
3. The data logger was set up, and the hammer and accelerometers were connected to the data logger to start knocking, as shown in Figure 9.

The frequencies of the structures can be obtained from the time history of the acceleration response by using fast Fourier transform (FFT). The accelerometers were installed, and the response signals were administeredusingan eight-channelsignal analyzer called OROS. The equipment was used to convert input analog signals to digital form

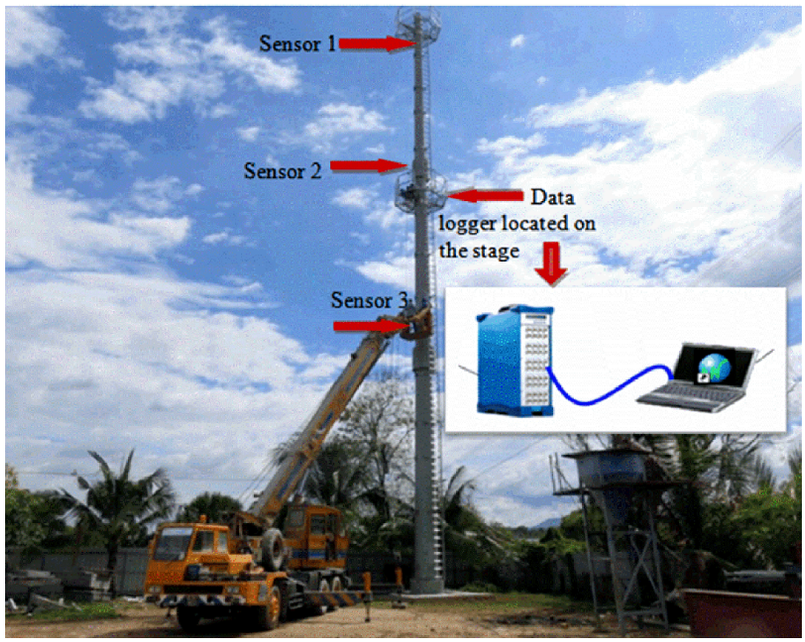

(a) Setup the data logger at real tower

(b) Knock different points on the tower

Figure 9. Experimental modal test of UHFPRC communication tower

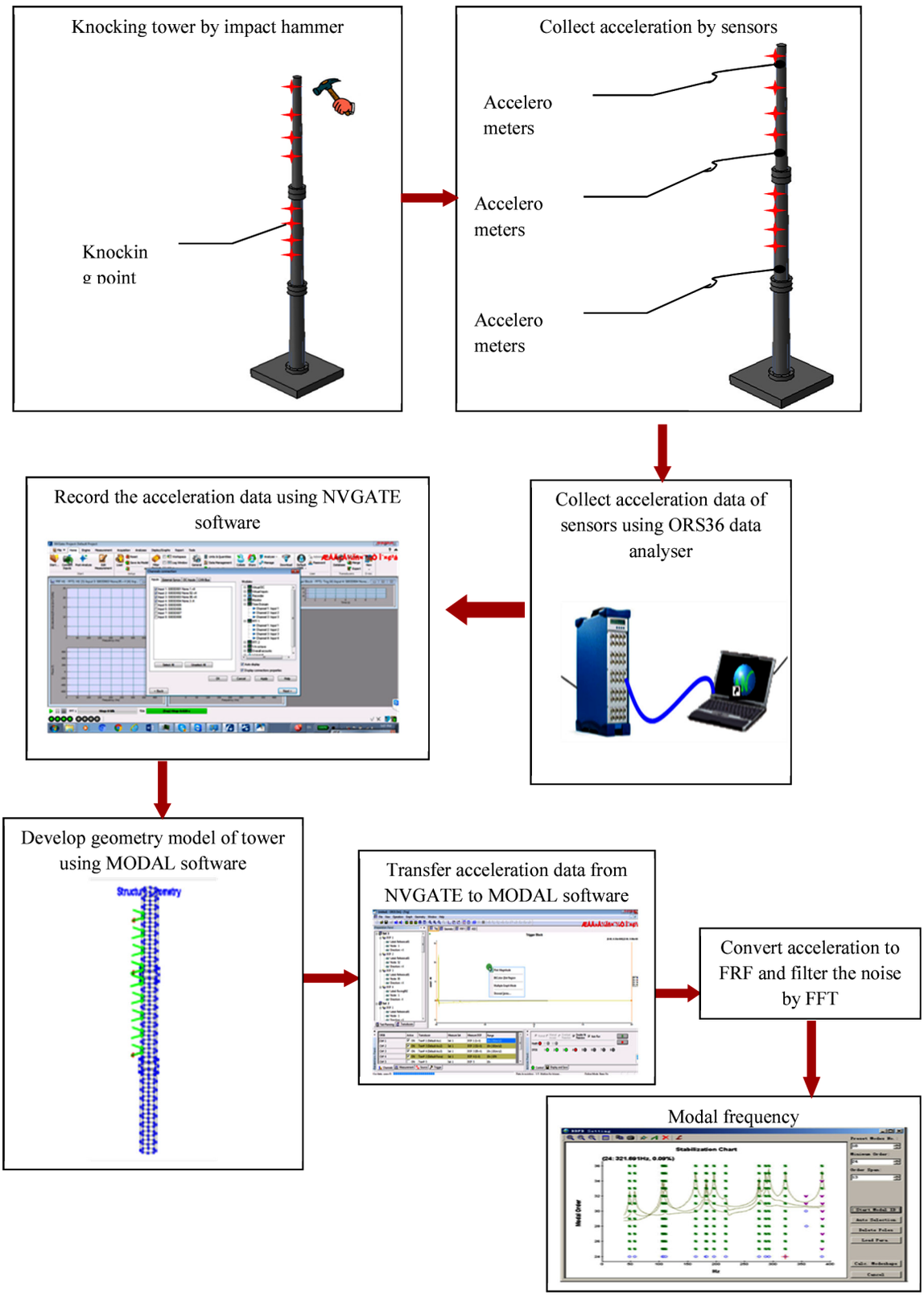

Figure 10. Functions for FRF Generation for UHPFRC communication tower

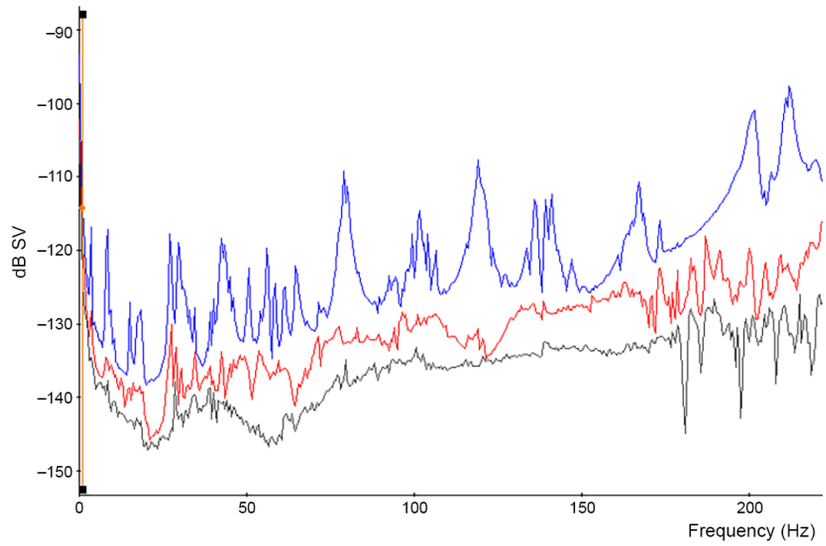

Figure 11. FRFs recorded at different accelerometer points for UHFPRC tower

through transducers. The data were recorded in the analyzer, and then converted to FFT using NVGATE software (Oros Gmbh, 2006). Then, NVGATE software exported the FFT results in universal file format (UFF). The MODAL utility program read the UFF files and exported them as frequency response function (FRF) files. The acceleration data corresponded to a frequency signal bandwidth of 400 Hz with 22 FRF data points. The sampling frequency was considered as 400 (sampling interval time was set as 0.0025 seconds) and the measured signal duration was set as 2 seconds. The resolution of the estimation was made by data analyzer and Modal Software during test data and its functioning to setup the data acquisition. From the experimental modal analysis, the dynamic properties of the tower, including the FRFs and natural frequencies, were determined during each healthy state. The modal analysis procedure for the UHPFRC communication tower is presented in Figure 10.

Table 1 shows the average frequency values determined in the dynamic tests for the tower on site. These values were used to verify the numerical analysis results. The frequency peak was 0.9 Hz, with the highest at 138.49 Hz. In accordance with the Eurocodes EN 1991-1-4 (CEN, 2005), EN 1993-3-1 (CEN, 2006), AS/NZS 1170.2 (Joint Technical Committee, 2004), resonant response is important when the first natural frequency of the structure is below 1 Hz. Therefore, dynamic analysis must be conducted to determine resonance response compared with background response. Resonant frequency must be considered when tracking the changes in the frequency, and it can be used as an indicator of damage.

Figure 11 shows the FRF graph recorded by three sensors. The different frequency peaks, which depicted the first 11 modes through the frequency bandwidth within the range of 0–400 Hz generated by MODAL software, were recorded. Thus, the maximum number of modes that can be captured with high precision through the selected setup is determined.

6. Validation of FEM

Experimental analysis was conducted to evaluate and verify the numerical frequency response of the 30 m tall communication tower under healthy condition for the first 11 modes, as listed in Table 1.

A convergence study was conducted to verify the material properties and meshing size of the suggested FEMs of the UHPFRC communication tower used in the optimization process.

The first 11 vibration modes before damage was obtained from the modal experimental test were compared with the first 11 modes of the FEMs. The results indicated that the maximum variation obtained in the frequencies from FEM and the experimental results was 5.6% for the UHPFRC communication tower. The difference in variation was less than 20% for all the results of the full-scale tower, there by proving that ABAQUS software is an appropriate tool for predicting the behavior of UHPFRC communication towers.

7. Development of the PSO algorithm for the correlation factor of damage frequency of UHPFC communication tower

The optimization technique was applied to generate an optimized correlation factor of the damage frequency of a communication tower. Three major points were considered before optimizing the damage frequency correlation ratio:

1) Formulation of the objective function;
2) Use of the PSO technique to optimize the damage frequency correlation ratio;
3) Use of convergence criteria (all the parameters are described in the following section).

7.1. Objective function

In this study, the PSO algorithm was used to optimize the correlation factor of damage frequency of communica-

tion tower and to determine the optimal values for the unknown set of coefficients, F_1, F_2 and F_3, from the solution space. A small difference was noted between the actual values and the predicted by applying the final optimized algorithm. Moreover, the convergence of the current method was determined by terminating the search process after identifying the set of coefficients that was able to minimize the objective function. MATLAB programming software was used to simulate and optimize the proposed damage frequency correlation ratio. The mean absolute error (*MAE*) objective function was used as follows (Hanoon, Jaafar, Hejazi, & Abdul Aziz, 2017a):

$$MAE = \frac{1}{n}\sum_{i=1}^{n}\left|f_{dactual} - f_{d\,pred}\right|, \quad (3)$$

where $f_{d\,pred}$ is the predicted value of the damage frequency of the communication tower, $f_{dactual}$ is the actual value of the damage frequency of the communication tower, and n is the number of data samples.

Different damage scenarios were created using FEM (see Appendix, Tables A.1–A.3). The damages consisted of sixty 200 mm cracks (30 vertical and 30 horizontal cracks at 1 m intervals), as shown in Figure 12. Then, damage types and locations were set as the damage index from Cases 0 to 6.

The proposed process was simulated using MATLAB to optimize the frequency of damage. This correlation factor can be determined using the following equation:

$$f_{Damaged} = c_1 \times \left(F_1 \times DI^2 + F_2 \times DI + F_3\right) \times f_{Healthy}, \quad (4)$$

where $f_{Damaged}$ and $f_{Healthy}$ are the frequencies under the damaged and healthy conditions of the tower. c_1 is a constant that depends on the mode number. F_1, F_2, and F_3 are the unknown coefficients. *DI* is the damage index (types and locations of damage), which is defined as:

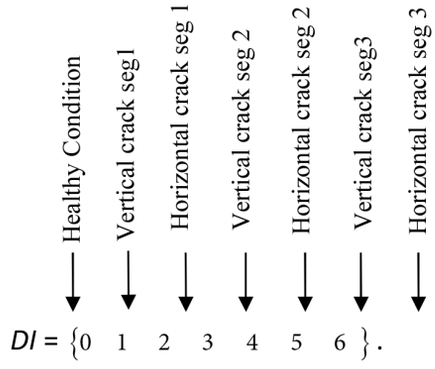

7.2. PSO algorithm

The initial PSO technique is a form of evolutionary computation process that was first proposed by Eberhart and Kennedy (1995).This technique is based on the social behavior of birds (particles), i.e. flocking. PSO is widely used because of its robustness, global convergence capability, and easy implementation (Xie, Wang, & Li, 2012; Chagwiza, Jones, Hove-Musekwa, & Mtisi, 2018).

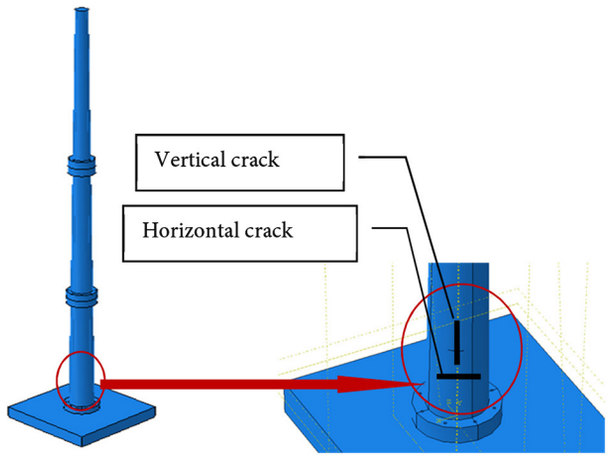

Figure 12. Vertical and horizontal crack for UHPFC communication tower

As discussed earlier, the PSO algorithm has been applied to a variety of optimization problems. In PSO, Eqns (5) and (6) (Kulkarni & Venayagamoorthy, 2011) are used to update the velocity and location of every particle while conducting the search process. Shi and Eberhart (1998) suggested using inertial weight (*w*) to improve the convergence rate of the PSO algorithm. Using the inertial weight helps set the particle contribution rate from their previous velocity value to their current velocity value. Through the entire search process, the velocity and position of every particle can be updated as:

$$V_i(t+1) = w \times V_i(t) + c_1 \times \mathrm{Rand}(\cdot)_1 \times \left[pbest_i(t) - X_i(t)\right] + c_2 \times \mathrm{Rand}(\cdot)_2 \times \left[gbest_i(t) - X_i(t)\right]; \quad (5)$$

$$X_i(t+1) = X_i(t) + V_i(t+1), \quad (6)$$

where V_i and X_i refer to the velocity and location of the studied particles, respectively; $\mathrm{Rand}(\cdot)_1$ and $\mathrm{Rand}(\cdot)_2$ represent the random numbers that are uniformly distributed from 0 to 1 and are regarded to be generally equal; c_1 and c_2 refer to the acceleration coefficients; pbest refers to the best location for every particle under study; and *gbest* denotes the best global position for all the studied particles. The acceleration coefficients denote the "trust" settings that indicate the degree of confidence in the best solution obtained by individual particles (cognitive parameter) or by the entire particle swarm (c_2 , social parameter). In Eqn (3), w refers to the inertial weight, which is a scaling factor that helps control the exploratory ability of the entire swarm and also scales the existing velocity value that influences the revised value of the velocity vector. The original PSO algorithm (Eberhart & Kennedy, 1995) does not contain the inertial weight because this was introduced later by Hanoon et al. (2017a) to improve the convergence rate.

Figure 13 describes the particle velocities and the revised positions for the 2D parameter space (Hanoon, Jaafar, Hejazi, & Abdul Aziz, 2017b). Here, the particle velocity contains three major vectors. Vector 1 is the mo-

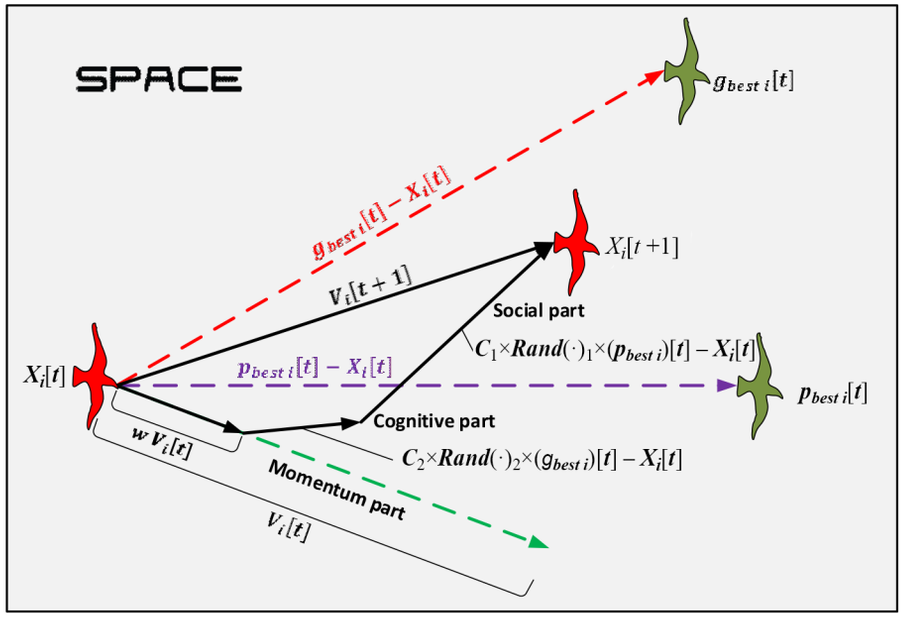

Figure 13. Description of the velocity and position updates in PSO for a two-dimensional parameter space

mentum or the inertial component that depends on the velocity of the particle at a previous stage. This vector enables the particle to continue along its existing trajectory. Vector 2 represents a cognitive or a memory component, which is derived based on the best particle position during all the iterations. This vector helps attract particles to their previous best position within the solution space. Finally, Vector 3 is the social or swarm component, which helps particles gravitate to the best positions in the swarm.

7.3. Convergence criteria

In accordance with the iterative nature of a PSO search, the application of convergence criteria will stop the optimization procedure. The two most widely used convergence criteria are the minimum error required to achieve the optimum value of the objective function (the degree of correlation between the frequency estimated by FEM and the frequency predicted by PSO) and the maximum iterations of the algorithm. The minimum error criterion assumes the previous information of the global optimum value, where as the nature of the optimization problem determines the maximum number of iterations. In the case of prior knowledge of the optimum value, mathematical algorithms can be used to resolve the problems. However, these methods are inapplicable to practical structural optimization issues without prior information of the optimum value.

The main PSO parameters identified by Hanoon et al. (2017a) are listed in Table 2, and the convergence criteria used in the PSO in this research are listed in Table 3.

8. Implementing PSO for predicting the correlation factor of damage frequency of UHPFRC communication tower

Applying the PSO algorithm helps determine the optimized solution by calculating the best and optimal values for the unknown coefficients of F_1, F_2, and F_3, which consequently helps improve the performance of the damage frequency correlation ratio. In this study, we incorporated the PSO algorithm to create a correlation factor of the damage frequency of a communication tower that was expected to decrease the errors between the actual

Table 2. Main PSO parameters

Description	Details
N is particles number	A typical range is 10–40. For some complicated or special problems, the number can be increased to 50–100.
D is particles Dimension	It is determined by the problem to be optimized.
W is the weight of Inertia	Usually is set to a value less than 1, and for faster convergence, $w = 0.7$ is considered (Lavanya & Udgata, 2011). It can also be updated during iterations.
Vectors containing the lower and higher bounds of the n design variables, respectively, xL, xU	They are determined by the problem to be optimized. Different ranges for different dimensions of particles can be applied in general.
Cognitive and social parameters	Usually $c_1 = c_2 = 1.494$ (Lavanya & Udgata, 2011). Other values can also be used, provided that $0 < c_1 + c_2 < 4$.

Table 3. PSO convergence parameters

Description	Details
T_{max} is the maximum value of iterations for the termination criterion.	Obtained by the complexity of the problem to be optimized, in coupling with other PSO parameters (D, N).
k_f is the value of iterations for which the relative improvement of the objective function satisfies the convergence check.	If the relative enhancing of the objective function over the last k_f iterations (containing the current iteration) is less or equal to f_m, convergence has been completed.
f_m is minimum relative to enhancing the number of the objective function.	

and predicted values. We implemented the PSO algorithm using MATLAB. Every swarm present in the PSO algorithm contained the F_1, F_2, and F_3 coefficients. The obtained values of the unknown coefficients were used in the proposed damage frequency correlation ratio to decrease the errors in estimating the correlation factor of the damage frequency values. Figure 14 shows the flowchart of the proposed damage frequency correlation ratio, which was used to improve the accuracy of the correlation factor of damage frequency prediction. This chart shows the major structure of the correlation factor of the damage frequency.

The PSO algorithm can be implemented to search for the optimum correlation factor of the damage frequency of a communication tower through the following steps:

- The swarm is initialized by assigning a random position in the problem hyperspace to each particle;
- The objective function of the proposed damage frequency correlation ratio for each particle is evaluated;
- The objective function value of each individual particle is obtained by comparing the current value with its . If the current value is better than its, the present particle position, X_i, is set as $pbest_i$;
- The particle with the best objective function value is identified. The value of its objective function is determined as gbest, and its position is $gbest_i$;
- The positions and velocities of all the particles are updated using Eqns (5) and (6);
- Steps 2 to 5 are reiterated until the convergence criteria are satisfied (when the maximum number of iterations or a sufficiently good objective function value is reached).

8.1. Construction of the proposed PSO algorithm

A correlation factor, which is a simple procedure, was used to identify the relationship between the frequencies under healthy and damaged conditions of UHPFRC communication towers using PSO. Statistical analysis methods, including the coefficient of variation (CoV) and correlation coefficient (R) analysis, were used in this study to evaluate or test the frequency correlation factor for a damaged UHPFRC communication tower. The mean square error (MSE) objective function was used in this study.

The amount of data utilized to build a particular model can adversely affect the accuracy of the final model. The

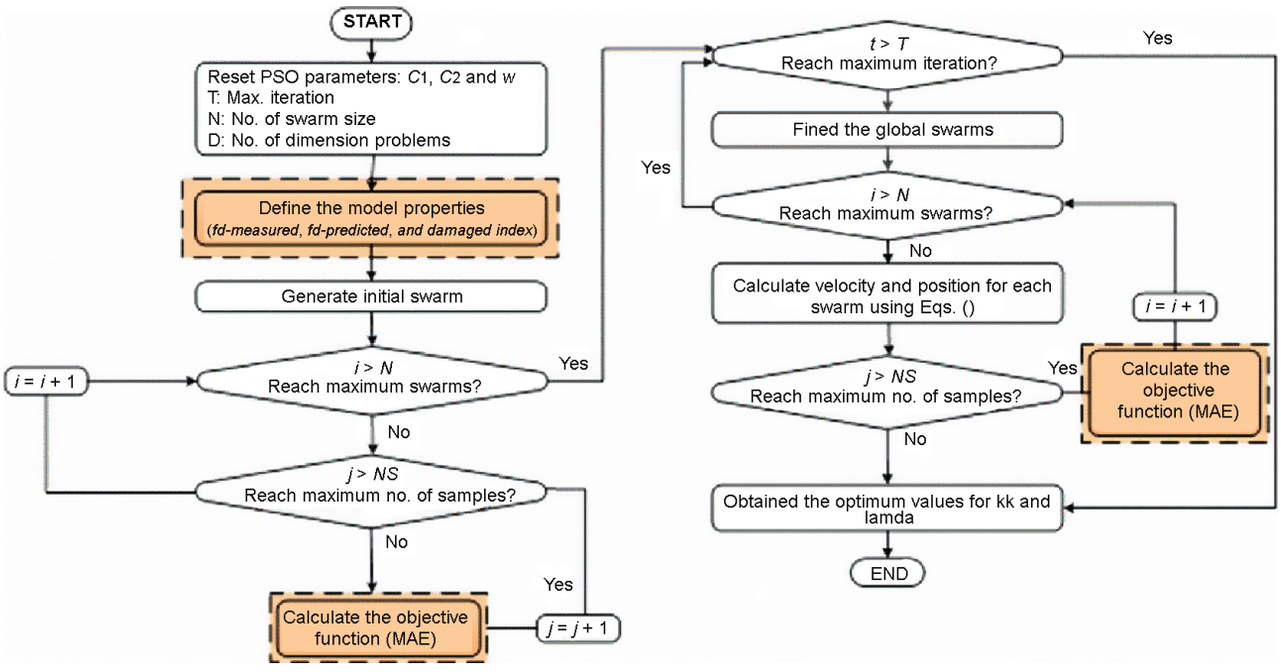

Figure 14. Flowchart of hybrid PSO for calculating correlation factor of the frequency of damage communication tower

minimum ratio of swarm sizes is estimated from the number of objects over the number of selected variables. Model acceptability was originally suggested by Frank and Todeschini (1994).They further suggested that five swarms will be safer than three swarms. In the current research, this ratio was considerably higher, with a value of 60/2, which is equal to 30 swarms.

The values of $c_1 = c_2 = 1.494$ (cognitive and social acceleration factors) and $w = 0.7$ (initial inertia weight) were suggested by Lavanya and Udgata (2011) to achieve rapid convergence. These values were used in the current investigation.

The process involved in the PSO algorithm is updated until a predefined number of maximum iterations is reached or a suitable *gbest* is generated. In this study, the number of iterations was estimated to be 5000 because of the variation in the objective functions that becomes constant after 2800 iterations. Five swarm sizes (10, 20, 30, 40, and 50) were investigated to enable the PSO algorithm to select suitable swarms that can minimize the elapsed time and error. The PSO algorithm was tested for the PSO parameters, and the following objective functions of MSE were obtained for 10, 20, 30, 40, and 50 swarms. Figure 15 illustrates that 30 swarms yield the best solution in the algorithm, which indicates the minimum objective functions of 0.00261 for MSE. On one hand, as warm size of 30 yields more optimum results in terms of computation time and accuracy based on the pre-analysis result of different swarm sizes.

On the other hand, swarm sizes of 10 and 20 exhibited high error rates, and swarm sizes of 40 and 50 required longer analysis times than that of a swarm size of 30, which achieved a minimum objective function. The optimum values for the unknown coefficients F_1, F_2, and F_3 obtained from the algorithm are presented in Table 4, and are applied in the proposed damage frequency correlation ratio. In accordance with a logical hypothesis introduced by Smith and Shust (2004), when the correlation coefficient (Figure 16) of a model exceeds 0.8, a strong correlation exists between the predicted frequency by the PSO algorithm and the estimated frequency value by FEM. Figure 15 shows that the proposed damage frequency correlation ratio with a high R (0.871) value predicted the target values with an acceptable accuracy degree.

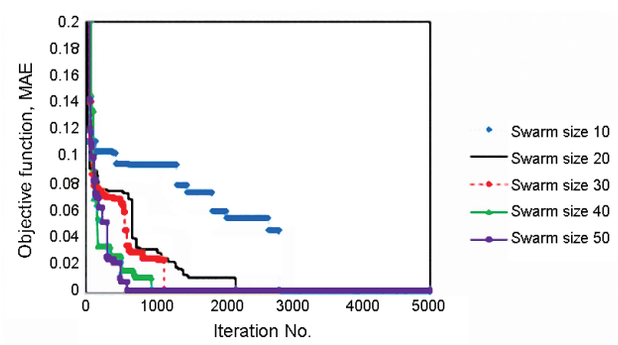

Figure 15. Convergence process for different swarm sizes

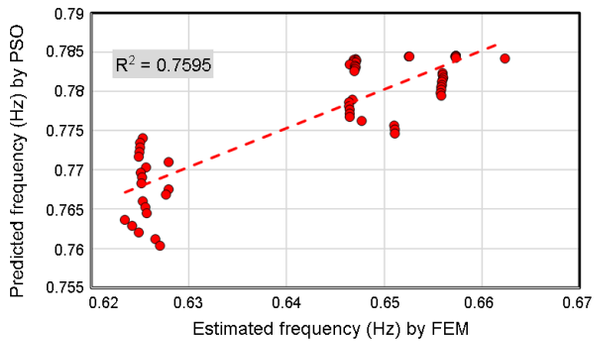

Figure 16. Estimated frequency by FEM vs. predicted frequency by PSO correlation factor for the frequency of damage UHFPRC communication tower

Table 4. Parameters used in the PSO algorithm setting

Factor	Value
F_1	-8.3757×10^{-6}
F_2	7.4987×10^{-5}
F_3	0.8378
Iteration	5000
Upper bound	1
Lower bound	–1

The proposed damage frequency correlation ratio that predicts the damage frequency of a UHPFRC communication tower using PSO is given by the following Eqn:

$$f_{damage} = ((-8.3757 \times 10^{-6} \times DI^2) + (7.4987 \times 10^{-5} \times DI) + 0.8378) \times f_{healthy}, \quad (7)$$

where f_{damage} – damage frequency of the tower; $f_{healthy}$ – healthy frequency of the tower; DI – damage index.

9. Verification of the proposed damage frequency correlation ratio with case studies

The FEM for the 30 m tall communication tower determined the frequency response that was produced to build the PSO algorithm for developing the damage correlation factor. Two case studies were considered to validate the proposed damage frequency correlation ratio.

9.1. Case study 1

A 15 m tall communication tower was constructed to validate the proposed damage frequency correlation ratio for the correlation factor of frequency of the damaged UHPFRC communication tower. Figure 17 shows the comparisons of the damage frequency correlation ratio f_d predicted using PSO and the damage frequency correlation ratio f_{damage} estimated through FEM with the damage index, which consists of 60 types of damage, there by proving that the proposed damage frequency correla-

tion ratio is generally trustworthy. Previous studies have showed that a *CoV* value below 10% indicates high accuracy as reported by Gomes (2000), whereas *CoV* values between 20% and 30% signify low accuracy, and values above 30% represent low precision. In this study, the *CoV* values were 0.94%, 0.95%, and 1.12% for the first three vibration modes, thereby indicating that the predicted results of the proposed damage frequency correlation ratio exhibit high accuracy and consistency. The mean value achieved in the proposed damage frequency correlation ratio of the correlation factor of the frequency of the damaged UHPFRC communication tower is close to 1.0 (1.1), which indicates good correlation between the estimated and measured frequencies of the damaged communication tower. Therefore, the proposed damage frequency correlation ratio efficiently estimated the frequency of the damaged communication tower, by considering different geometries and material properties.

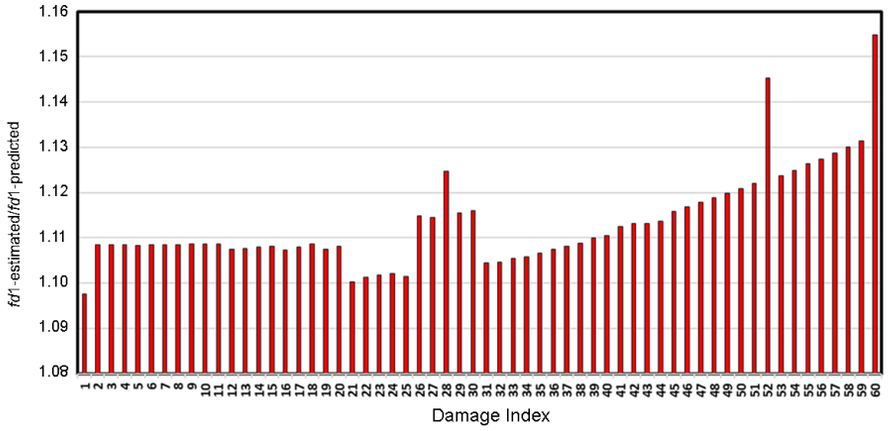

(a) Predictions and estimated of frequency for damaged communication tower for the first mode

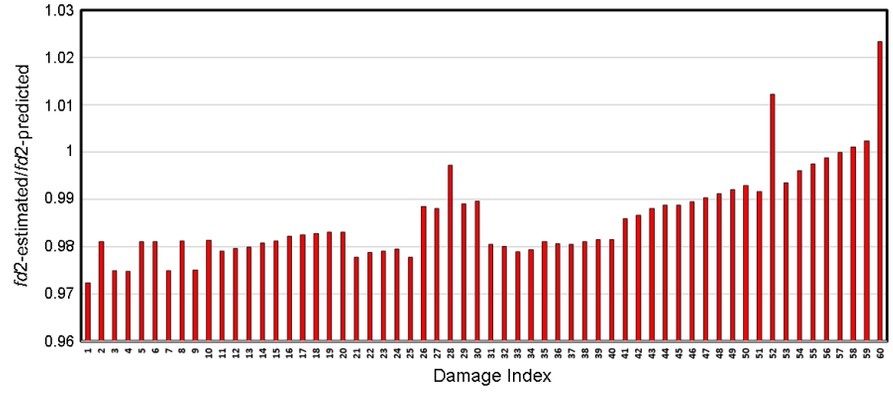

(b) Predictions and estimated of frequency for damaged communication tower for the second mode

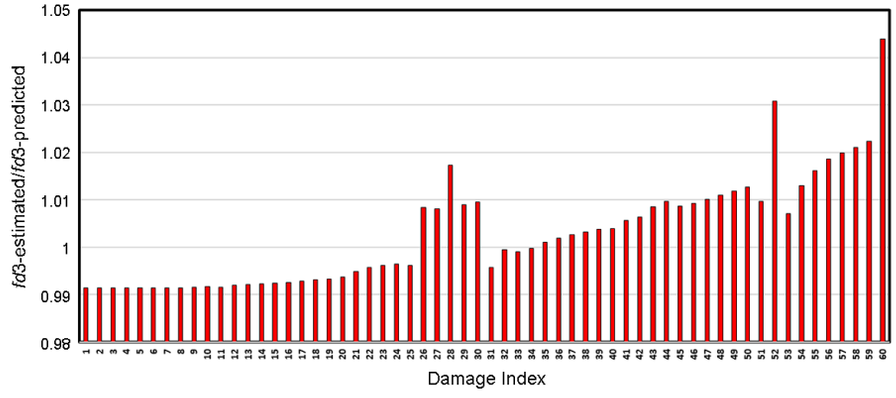

(c) Predictions and estimated of frequency for damaged communication tower for the third mode

Figure 17. Comparisons between the predictions and measured of frequency for tower damaged with 15 m height

9.2. Case study 2

Another communication tower with a height of 45 m was simulated using FEM to verify the proposed damage frequency correlation ratio for the correlation factor of the frequency of the damaged UHPFRC communication tower. Figure 18 displays the comparison of the f_{damage} predicted using PSO and f_{damage} measured through FEM with the damage index, which consists of 60 types of damage. The proposed damage frequency correlation ratio achieved reliable and trustworthy results because the mean values of the MSE and root MSE are significantly near 1.0. The coefficients of variation obtained from the results of the proposed damage frequency correlation ratio are 3.8%, 1.7%, and 0.98%, which indicate the good accuracy and consistency of the obtained values. The results were sufficient to consider the proposed damage frequency correlation ratio in properly assessing the frequency of the damaged communication tower. Moreover, further research is necessary to improve the accuracy level of the proposed damage frequency correlation ratio for the correlation factor of the frequency of the damaged UHPFRC communication tower.

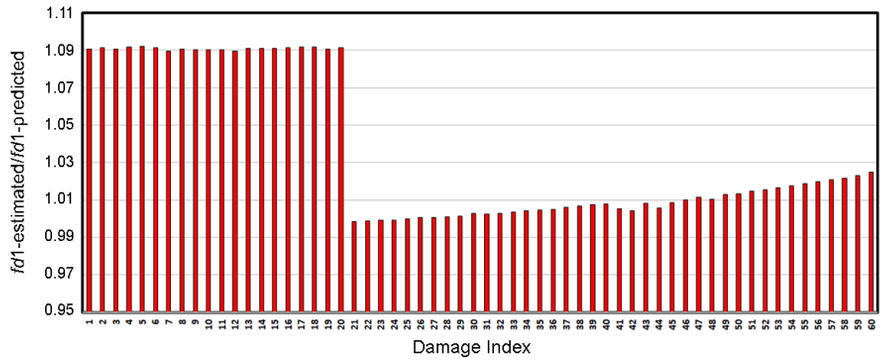

(a) Predictions and estimated of frequency for damaged communication tower for the first mode

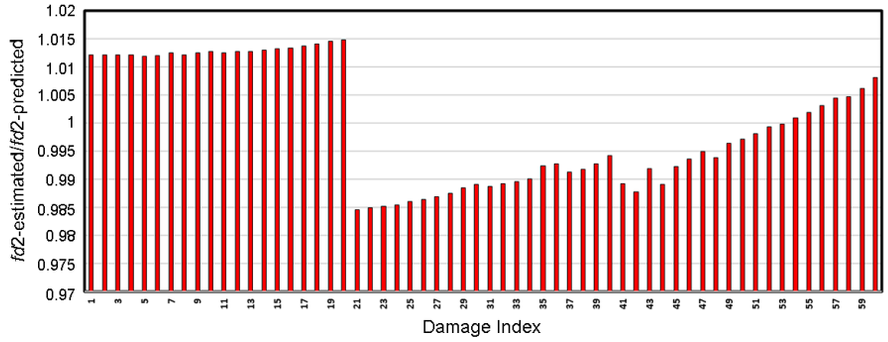

(b) Predictions and estimated of frequency for damaged communication tower for the second mode

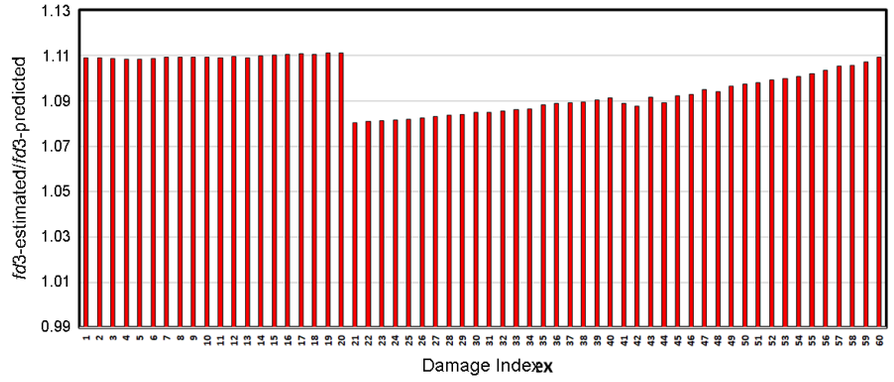

(c) Predictions and estimated of frequency for damaged communication tower for the third mode

Figure 18. Comparisons between the predictions and measured of frequency for a damaged tower with a 45 m height

Conclusions

This study proposed a correlation factor for identifying the relationship between frequencies underhealthy and damaged states of various UHPFRC communication towers under different configurations using PSO. FEM was implemented to predict the behavior of a communication tower under healthy and damaged conditions through a dynamic frequency that contributed to building and testing the PSO algorithm. Three communication towers with heights of 15 m, 30 m, and 45 m were considered to develop the frequency correlation factor. The tower with a height of30m was tested experimentally to verify the results and develop the PSO algorithm for the damage correlation, whereas the towers with the heights of 15 m and 45 m were used to validate the algorithm.

On the basis of the results of the preceding case studies, the following conclusions were drawn:

- The maximum variation in the frequencies obtained from FEM and the experimental results was 5.8% for a UHPFRC communication tower.
- The first natural frequency considerably changed compared with the other natural frequencies after damage occurred. The changes in frequency after damage depended on the span, geometry, and level of damage suffered by the structure. The variation in low frequencies due to damage formation in the tower is more evident than that in high frequencies, which exhibits less variation, and identifying the changes in frequencies for different types and locations of damage can be complicated.
- The damage frequency correlation ratio was based on the data collected from three simulated FEMs of communication towers.
- A wide range of datasets with a total of 540 from the three simulated FEMs of the communication towers was used to build and verify the correlation factor of the damage frequency of a tower. The statistical analysis showed that the *CoV*, mean, and *R* values achieved good accuracy and consistency with the obtained values. Therefore, the correlation factor can be widely used to predict the damage frequency of communication towers.
- The 15m-tall tower presented *CoV* values of 0.94%, 0.95%, and 1.12% for the first three modes, thereby indicating that the predicted results of the proposed damage frequency correlation ratio exhibited high accuracy and consistency. Meanwhile, the 45 m tall tower presented *CoV* values of approximately 3.8%, 1.7%, and 0.98% for the first three modes, which indicates good correlation between the measured and estimated damage frequencies of the communication tower obtained using the proposed damage frequency correlation ratio.

Acknowledgements

This research receives support from Dura Technology Sdn. Bhd. and Dr. Voo Yen Lai, under a research project from Ministry of Science Technology & Innovation, Malaysia, entitled "Development and construction of Internet Transmission Tower Using Ultra High-Performance Concrete". Their help and support are gratefully acknowledged.

Author contributions

Authors made substantial contributions to acquisition of data and analysis and interpretation of data; participated in drafting the article; and gave final approval of the version to be submitted and any revised version.

Funding

This work was supported by the Dura Technology Sdn. Bhd through Dr. Voo Yen Lai under Research Project from Mosti (Ministry of Science Technology & Innovation).

Disclosure statement

The authors declare that they have no relevant or material financial interests that relate to the research described in this paper.

References

Alaghebandha, M., Hajipour, V., & Hemmati, M. (2017). Optimizing multi-objective sequencing problem in mixed-model assembly line on just-in-time: particle swarm optimization algorithm. *International Journal of Management Science and Engineering Management*, *12*(4), 288-298. https://doi.org/10.1080/17509653.2016.1258593

Antunes, P., Travanca, R., Varum, H., & André, P. (2012). Dynamic monitoring and numerical modelling of communication towers with FBG based accelerometers. *Journal of Constructional Steel Research*, *74*, 58-62. https://doi.org/10.1016/j.jcsr.2012.02.006

Ashour, A. F., & Rishi, G. (2000). Tests of reinforced concrete continuous deep beams with web openings. *ACI Structural Journal*, *97*(3), 418-426.

Begambre, O., & Laier, J. E. (2009). A hybrid Particle Swarm Optimization–Simplex algorithm (PSOS) for structural damage identification. *Advances in Engineering Software*, *40*(9), 883-891. https://doi.org/10.1016/j.advengsoft.2009.01.004

Chagwiza, G., Jones, B. C., Hove-Musekwa, S. D., & Mtisi, S. (2018). A new hybrid matheuristic optimization algorithm for solving design and network engineering problems. *International Journal of Management Science and Engineering Management*, *13*(1), 11-19. https://doi.org/10.1080/17509653.2016.1269136

Dassault Systèmes Simulia Corp. (2014). *ABAQUS standard user's manual*. Version 6. RI, USA: Providence,. RI, USA.

Dong, R., Xu, J., & Lin, B. (2017). ROI-based study on impact factors of distributed PV projects by LSSVM-PSO. *Energy*, *124*, 336-349. https://doi.org/10.1016/j.energy.2017.02.056

Dua, R., Watkins, S. E., Wunsch, D. C., Chandrashekhara, K., & Akhavan, F. (2001, July). Detection and classification of impact-induced damage in composite plates using neural networks. In *Proceedings of the International Joint Conference on Neural Networks* (IJCNN'01), 15–19 July 2001, Washington, DC, USA. https://doi.org/10.1109/IJCNN.2001.939106

Eberhart, R., & Kennedy, J. (1995, October). A new optimizer using particle swarm theory. In *Proceedings of the Sixth International Symposium on the Micro Machine and Human Science (MHS'95)*, 4–6 October 1995, Nagoya, Japan. https://doi.org/10.1109/MHS.1995.494215

European Committee for Standardization (CEN). (2005). *EN 1991-1-4, Eurocode 1: Actions on structures, part 1–4: general actions – wind actions*.

European Committee for Standardization (CEN). (2006). *EN 1993-3-1, Eurocode 3: Design of steel structures, part 3–1: towers, masts and chimneys – towers and masts*.

Frank, I. E., & Todeschini, R. (1994). *The data analysis handbook*. Vol. 14. Amsterdam, Netherlands: Elsevier.

Gomes, F. P. (2000). *Experimental statistics*. Piracicaba: FEALQ (in Portuguese).

Grünbaum, C. (2008). *Structures of tall buildings* (Rapport TVBK-5156). Lund: Lunds Tekniska Högskola.

Guidorzi, R., Diversi, R., Vincenzi, L., Mazzotti, C., & Simioli, V. (2014). Structural monitoring of a tower by means of MEMS-based sensing and enhanced autoregressive models. *European Journal of Control*, *20*(1), 4-13. https://doi.org/10.1016/j.ejcon.2013.06.004

Hanoon, A. N., Jaafar, M. S., Hejazi, F., & Abdul Aziz, F. N. (2017a). Strut-and-tie model for externally bonded CFRP-strengthened reinforced concrete deep beams based on particle swarm optimization algorithm: CFRP debonding and rupture. *Construction and Building Materials*, *147*, 428-447. https://doi.org/10.1016/j.conbuildmat.2017.04.094

Hanoon, A. N., Jaafar, M. S., Hejazi, F., & Abdul Aziz, F. N. (2017b). Energy absorption evaluation of reinforced concrete beams under various loading rates based on particle swarm optimization technique. *Engineering Optimization*, *49*(9), 1483-1501. https://doi.org/10.1080/0305215X.2016.1256729

Joint Technical Committee. (2002). *AS/NZS 1170.2 Structural design actions, Part 2: wind actions*. Australian/New Zealand Standard. Sydney: Standards Australia International Ltd and Wellington: Standards New Zealand.

Kaveh, A., & Zolghadr, A. (2015). An improved CSS for damage detection of truss structures using changes in natural frequencies and mode shapes. *Advances in Engineering Software*, *80*, 93-100. https://doi.org/10.1016/j.advengsoft.2014.09.010

Kazemi, M. A., Nazari, F., Karimi, M., Baghalian, S., Rahbarikahjogh, M. A., & Khodabandelou, A. M. (2011, April). Detection of multiple cracks in beams using particle swarm optimization and artificial neural network. In *The 4th International Conference on Modeling, Simulation and Applied Optimization (ICMSAO)*, 19–21 April 2011, Kuala Lumpur, Malaysia. https://doi.org/10.1109/ICMSAO.2011.5775595

Kessler, S. S., Spearing, S. M., Atalla, M. J., Cesnik, C. E. S., & Soutis, C. (2002). Damage detection in composite materials using frequency response methods. *Composites Part B: Engineering*, *33*(1), 87-95. https://doi.org/10.1016/S1359-8368(01)00050-6

Kim, J-T., & Stubbs, N. (2002). Improved damage identification method based on modal information. *Journal of Sound and Vibration*, *252*(2), 223-238. https://doi.org/10.1006/jsvi.2001.3749

Kulkarni, R. V., & Venayagamoorthy, G. K. (2011). Particle swarm optimization in wireless-sensor networks: A brief survey. *IEEE Transactions on Systems, Man, and Cybernetics, Part C (Applications and Reviews)*, *41*(2), 262-267. https://doi.org/10.1109/TSMCC.2010.2054080

Lavanya, D., & Udgata, S. K. (2011). Swarm intelligence based localization in wireless sensor networks. In the *International Workshop on Multi-disciplinary Trends in Artificial Intelligence*. https://doi.org/10.1007/978-3-642-25725-4_28

Majumdar, A., Nanda, B., Maiti, D. K., & Maity, D. (2014). Structural damage detection based on modal parameters using continuous ant colony optimization. *Advances in Civil Engineering*, Article ID 174185. https://doi.org/10.1155/2014/174185

Mhaske, M. S., & Shelke, R. S. (2015). Detection of depth and location of crack in a beam by vibration measurement and its comparative validation in ANN and GA. *International Engineering Research Journal (IERJ)*, Special Issue 2, 488-493.

Negm, H. M., & Maalawi, K. Y. (2000). Structural design optimization of wind turbine towers. *Computers & Structures*, *74* (6), 649-666. https://doi.org/10.1016/S0045-7949(99)00079-6

Nhamage, I. A., Lopez, R. H., & Miguel, L. F. F. (2016). An improved hybrid optimization algorithm for vibration based-damage detection. *Advances in Engineering Software*, *93*, 47-64. https://doi.org/10.1016/j.advengsoft.2015.12.003

Oros Gmbh. (2006). *3-Series/NVGate reference manual*.

Paultre, P., Weber, B., Mousseau, S., & Proulx, J. (2016). Detection and prediction of seismic damage to a high-strength concrete moment resisting frame structure. *Engineering Structures*, *114*, 209-225. https://doi.org/10.1016/j.engstruct.2016.02.013

Rardin, R. L. (1998). *Optimization in operations research*. New York: Prentice Hall.

Ren, W.-X., & De Roeck, G. (2002). Structural damage identification using modal data. II: Test verification. *Journal of Structural Engineering*, *128*(1), 96-104. https://doi.org/10.1061/(ASCE)0733-9445(2002)128:1(96)

Saisi, A., Gentile, C., & Guidobaldi, M. (2015). Post-earthquake continuous dynamic monitoring of the Gabbia Tower in Mantua, Italy. *Construction and Building Materials*, *81*, 101-112. https://doi.org/10.1016/j.conbuildmat.2015.02.010

Shi, Y., & Eberhart, R. (1998). A modified particle swarm optimizer. In *Proceedings of the IEEE International Conference on the Evolutionary Computation, IEEE World Congress on Computational Intelligence*, 4–9 May 1998, Anchorage, AK, USA. https://doi.org/10.1109/ICEC.1998.699146

Sinou, J.-J. (2009). *A review of damage detection and health monitoring of mechanical systems from changes in the measurement of linear and non-linear vibrations*. Nova Science Publishers, Inc.

Smith, K. B., & Shust, W. C. (2004). Bounding natural frequencies in structures I: Gross geometry, material and boundary conditions. In *Proceedings of the XXII International Modal Analysis Conference, Society of Experimental Mechanics*.

Sutar, M. K. (2012). Finite element analysis of a cracked cantilever beam. *International Journal of Advanced Engineering Research and Studies*, *1*(2), 285-289.

Xie, F., Wang, Q-j., & Li, G-l. (2012). Optimization research of FOC based on PSO of induction motors. In *15th International Conference on Electrical Machines and Systems (ICEMS)*, 21–24 October 2012, Sapporo, Japan.

Yang, X. F., Swamidas, A. S. J., & Seshadri, R. (2001). Crack identification in vibrating beams using the energy method. *Journal of Sound and Vibration*, *244*(2), 339-357. https://doi.org/10.1006/jsvi.2000.3498

Appendix

Table A.1. Frequency results for tower with 15 m height

Description (Class)	segment	Case no.	freq 1	freq 2	freq 3	freq 4	freq 5	freq 6	freq 7	freq 8	freq 9	freq 10	freq 11	Damage index
Healthy	–	–	3.39125	14.1403	31.747	56.8703	63.74	79.0697	100.339	110.351	139.685	185.324	193.824	0
vertical crack	seg1	1	3.11861	12.9689	28.9676	28.9676	29.163	52.2058	58.6117	72.6925	91.6692	92.2513	127.809	1
	seg1	2	3.1498	13.0861	28.9707	29.1691	52.2039	58.7984	72.6935	91.8002	92.4274	101.267	127.822	1
	seg1	3	3.14979	13.0032	28.9706	29.1691	52.2023	58.7984	72.6935	91.8007	92.4277	101.266	127.826	1
	seg1	4	3.14978	13.0027	28.9704	29.1689	52.1806	58.3164	72.6933	91.8164	92.4277	101.259	127.846	1
	seg1	5	3.14977	13.0862	28.9704	29.1689	52.1767	58.3172	72.6933	91.8144	92.4276	101.258	127.831	1
	seg1	6	3.14976	13.0862	28.9703	29.169	52.1729	58.3178	58.7981	72.6932	91.8114	92.4276	128.354	1
	seg1	7	3.14977	13.0026	28.9703	29.169	52.1721	58.3177	72.6932	91.8118	92.4276	101.258	127.816	1
	seg1	8	3.1498	13.0858	28.97	29.1693	52.1659	58.3179	72.6944	91.8076	92.4274	101.257	127.804	1
	seg1	9	3.14973	13.0031	28.9702	29.1687	52.168	58.798	72.6926	91.81	92.4249	101.259	127.815	1
	seg1	10	3.1496	13.0858	28.9698	29.1669	52.1814	58.3146	72.6894	91.8118	92.4239	101.264	127.828	1
Horizontal crack	seg1	1	3.14911	13.0532	28.9642	29.1247	52.203	58.7126	72.6308	91.797	92.2907	101.265	127.805	2
	seg1	2	3.1452	13.0607	28.971	29.118	52.1949	58.3053	72.6025	91.7929	92.3527	101.259	127.799	2
	seg1	3	3.14528	13.0621	28.9711	29.1294	52.1926	58.3087	72.5974	91.796	92.3998	101.258	127.81	2
	seg1	4	3.14598	13.0705	28.9712	29.1608	52.1872	58.3136	72.5819	91.8079	92.4128	101.257	127.858	2
	seg1	5	3.14579	13.0745	28.9697	29.1667	52.1854	58.3117	72.5758	91.8094	92.3559	101.257	127.864	2
	seg1	6	3.14236	13.0843	28.9684	29.1499	52.15	58.2985	72.5034	91.8054	92.2441	101.243	127.819	2
	seg1	7	3.14368	13.0853	28.9689	29.1435	52.1554	58.3028	72.5157	91.8085	92.2666	101.248	127.813	2
	seg1	8	3.14491	13.086	28.9691	29.1231	52.1548	58.3069	72.513	91.8096	92.3073	101.25	127.8	2
	seg1	9	3.14069	13.0851	28.9667	29.0866	52.1207	58.2674	72.448	91.7957	92.3122	101.236	127.761	2
	seg1	10	3.14142	13.0811	28.9678	29.0371	52.1064	58.2591	72.4409	91.7905	92.3866	101.235	127.771	2
vertical crack	seg2	1	3.11824	13.0063	28.9921	29.1862	52.2292	58.2596	72.7324	91.7521	92.2658	101.275	127.925	3
	seg2	2	3.12013	13.0161	29.0107	52.2366	58.276	72.7454	91.8354	92.3566	101.354	127.963	128.594	3
	seg2	3	3.1202	13.0157	29.0096	52.236	58.2764	72.7453	91.8325	92.3529	101.339	127.957	128.588	3
	seg2	4	3.12021	13.0157	29.0089	52.2344	58.2789	72.7452	91.8266	92.3532	101.314	127.965	128.588	3
	seg2	5	3.11707	12.9874	28.99	52.2172	58.2598	72.7097	91.7373	92.0718	101.121	127.914	128.378	3
	seg2	6	3.15335	13.1235	29.3322	52.846	58.9421	73.566	92.8159	93.1545	102.34	129.42	129.891	3
	seg2	7	3.15089	13.1132	29.3084	52.8014	58.8963	73.5079	92.7357	93.0822	102.236	129.323	129.788	3
	seg2	8	3.17825	13.2277	29.5667	53.2756	59.411	74.1539	93.5474	93.898	103.143	130.459	130.929	3
	seg2	9	3.15087	13.1131	29.3084	52.7994	58.8947	73.5079	92.7339	93.0821	102.204	129.309	129.787	3
	seg2	10	3.15088	13.1137	29.3083	52.7962	58.8894	73.509	92.7406	93.1046	102.172	129.277	129.79	3

Continued Table A.1

Description (Class)	segment	Case no.	freq 1	freq 2	freq 3	freq 4	freq 5	freq 6	freq 7	freq 8	freq 9	freq 10	freq 11	Damage index
Horizontal crack	seg2	1	3.11661	12.9862	28.8937	29.1164	52.2107	58.2145	72.6423	91.4435	92.1204	101.093	127.619	4
	seg2	2	3.11537	12.9748	28.9859	29.1339	52.2267	58.6333	72.6767	91.7322	92.0429	101.251	127.898	4
	seg2	3	3.11579	12.9513	28.9589	29.1369	52.2192	58.6088	72.6647	91.5587	92.0313	101.159	127.883	4
	seg2	4	3.11506	12.95	28.9615	29.1498	52.2153	58.5255	72.6597	91.6408	92.0401	101.11	127.82	4
	seg2	5	3.11538	12.9647	28.9826	29.1729	52.2233	58.5134	72.6738	91.7517	92.1644	101.195	127.824	4
	seg2	6	3.11571	12.9511	28.989	29.1851	52.2235	58.4545	72.6717	91.736	92.2399	101.182	127.899	4
	seg2	7	3.11557	12.9406	28.9884	29.1611	52.2198	58.4852	72.6627	91.7315	92.2364	101.151	127.847	4
	seg2	8	3.11551	12.9384	28.9877	29.1556	52.2185	58.4803	72.6615	91.7285	92.214	101.132	127.863	4
	seg2	9	3.11676	12.9359	28.9839	29.1429	52.2176	58.5046	72.665	91.7163	92.081	101.112	127.888	4
	seg2	10	3.11609	12.9276	28.9658	29.0625	52.2101	58.5664	72.6482	91.557	91.8435	101.048	127.878	4
Vertical crack	seg3	1	3.11917	12.9764	28.9984	29.1967	52.2311	58.2546	72.7216	91.6987	92.2957	101.228	127.992	5
	seg3	2	3.11893	12.9748	28.9958	29.2063	52.2333	58.2696	72.72	91.6853	92.285	101.256	127.933	5
	seg3	3	3.11661	12.9834	29.0336	29.3632	52.228	58.2836	72.683	91.7284	92.3922	101.281	127.997	5
	seg3	4	3.11538	12.9832	29.0449	29.4004	52.2239	58.3036	72.6678	91.7554	92.4738	101.28	128.024	5
	seg3	5	3.11906	12.9722	28.9917	29.1876	52.2373	58.2798	72.7257	91.7426	92.324	101.275	127.976	5
	seg3	6	3.11896	12.9708	28.9869	29.1833	52.2377	58.2717	72.7256	91.7389	92.3358	101.28	127.995	5
	seg3	7	3.11928	12.9715	28.9857	29.18	52.2389	58.2637	72.7291	91.7182	92.2893	101.285	127.97	5
	seg3	8	3.1192	12.9706	28.9827	29.1772	52.2389	58.257	72.7287	91.7036	92.2828	101.286	127.951	5
	seg3	9	3.11941	12.9716	28.9843	29.1787	52.2395	58.2579	72.7307	91.7037	92.2794	101.289	127.95	5
	seg3	10	3.11929	12.9704	28.9803	29.1745	52.2393	58.2493	72.73	91.6906	92.2606	101.289	127.941	5
Horizontal crack	seg3	1	3.11973	12.9418	28.8689	29.0796	52.2392	58.2504	72.6978	91.6204	92.0498	101.259	127.544	6
	seg3	2	3.18096	13.1974	29.4439	29.6587	53.3009	59.4014	74.1417	93.4367	93.8746	103.319	130.079	6
	seg3	3	3.11828	12.9399	28.7388	29.0762	52.2314	57.8553	72.6962	91.6214	92.153	101.255	127.925	6
	seg3	4	3.11846	12.9606	28.8754	29.0778	52.2334	57.7253	72.7102	90.813	91.8925	101.258	127.625	6
	seg3	5	3.11906	12.9664	28.9384	29.1138	52.2339	57.928	72.7224	90.6078	91.9276	101.272	126.845	6
	seg3	6	3.11894	12.9689	28.9759	29.1538	52.2341	58.2246	72.7247	91.4362	91.9365	101.275	127.511	6
	seg3	7	3.11914	12.9705	28.9815	29.1657	52.2378	58.2405	72.7269	91.5513	92.04	101.282	127.691	6
	seg3	8	3.11931	12.9711	28.9835	29.1774	52.2387	58.2536	72.7297	91.6837	92.2657	101.287	127.918	6
	seg3	9	3.11959	12.9729	28.9883	29.182	52.2392	58.263	72.7321	91.7048	92.2789	101.29	127.947	6
	seg3	10	3.18082	13.2291	29.5657	29.7632	53.301	59.4143	74.1768	93.5229	94.1084	103.35	130.49	6

Table A.2. Frequency results for tower with 30 m height

Description (Class)	segment	Case no.	freq 1	freq 2	freq 3	freq 4	freq 5	freq 6	freq 7	freq 8	freq 9	freq 10	freq 11	Damage index
Healthy	–	–	0.93	0.94	3.8	8.87	17.79	20.1	41.35	74.15	104.14	113.86	137.44	0
Vertical crack	seg1	1	0.781604	3.16675	7.38986	14.8092	23.3101	30.8435	34.4437	46.9911	47.0116	61.7492	61.7892	1
	seg1	2	0.781639	3.1666	7.38927	14.8084	23.3092	30.8427	34.4416	46.9905	47.0091	61.7467	61.7863	1
	seg1	3	0.784496	3.17148	7.39981	14.8267	23.331	33.1532	34.476	47.0369	47.0573	61.8193	70.1399	1
	seg1	4	0.784494	3.17151	7.39987	14.8269	23.3321	33.1509	34.4788	47.0351	47.0592	61.8195	70.1293	1
	seg1	5	0.784486	3.17147	7.39991	14.8272	23.3327	33.1517	34.4795	47.0383	47.0592	61.8177	70.1317	1
	seg1	6	0.784474	3.17143	7.4	14.8276	23.3332	33.151	34.4786	47.0381	47.0571	61.8157	70.1287	1
	seg1	7	0.784438	3.1714	7.39995	14.8276	23.3333	33.1489	34.4782	47.0325	47.0561	61.816	70.12	1
	seg1	8	0.784477	3.17144	7.40005	14.8279	23.3332	33.1488	34.4769	47.0328	47.0567	61.8205	70.1197	1
	seg1	9	0.784491	3.17143	7.40011	14.828	23.3329	33.1491	34.4767	47.0388	47.0581	61.822	70.1209	1
	seg1	10	0.787484	3.17568	7.40652	14.84	23.3471	31.3487	34.4927	47.0594	47.0816	61.8586	63.6946	1
Horizontal crack	seg1	1	0.778324	3.1619	7.3846	14.7997	23.2973	26.3659	33.9216	34.4366	47.0049	54.0886	61.7264	2
	seg1	2	0.778219	3.16162	7.38413	14.7996	23.2982	26.3638	33.9209	34.4393	47.0079	54.091	61.7314	2
	seg1	3	0.778392	3.16194	7.38489	14.8014	23.3011	26.3687	33.9038	34.4429	47.0117	54.1063	61.7389	2
	seg1	4	0.778208	3.16169	7.38473	14.8015	23.3016	26.3658	33.9028	34.4449	47.0123	54.1107	61.7362	2
	seg1	5	0.778344	3.16187	7.38526	14.8026	23.3032	26.3694	33.8739	34.4462	47.0114	54.1253	61.7314	2
	seg1	6	0.77799	3.16099	7.3823	14.7966	23.294	26.3412	33.9226	34.4281	46.9908	54.0662	61.7029	2
	seg1	7	0.778292	3.16186	7.3855	14.8032	23.3033	26.3759	33.8927	34.4395	47.0015	54.1554	61.7217	2
	seg1	8	0.778355	3.16191	7.3855	14.8032	23.3024	26.3827	33.9084	34.4355	46.9991	54.1697	61.728	2
	seg1	9	0.778284	3.16189	7.38566	14.8031	23.3007	26.3821	33.9116	34.43	46.9975	54.1805	61.7324	2
	seg1	10	0.778259	3.16192	7.38562	14.8027	23.2995	26.3804	33.9051	34.427	46.9982	54.184	61.7326	2
Vertical crack	seg2	1	0.783679	3.16908	7.39697	14.8225	23.3206	26.4984	34.069	34.4374	34.4674	47.0131	47.0469	3
	seg2	2	0.783688	3.1694	7.39699	14.8235	23.322	26.4958	34.0677	34.4346	34.4692	47.0082	47.0455	3
	seg2	3	0.783716	3.16869	7.39759	14.8197	23.3229	26.4964	34.07	34.4298	34.4626	47.0069	47.0443	3
	seg2	4	0.783666	3.16962	7.39677	14.8237	23.3231	26.4969	34.0676	34.4241	34.4655	47.0158	47.0498	3
	seg2	5	0.783655	3.16909	7.39681	14.8218	23.3224	26.4961	34.0685	34.4253	34.4631	47.0175	47.0485	3
	seg2	6	0.783623	3.16992	7.39677	14.8239	23.3236	26.4916	34.0663	34.4244	34.4662	47.0021	47.0467	3
	seg2	7	0.783593	3.16981	7.39656	14.8236	23.3227	26.4871	34.0655	34.4186	34.466	46.9941	47.0442	3
	seg2	8	0.783578	3.16939	7.39623	14.8234	23.3204	26.4926	34.0662	34.4282	34.4659	47.0146	47.0458	3
	seg2	9	0.783551	3.16868	7.3962	14.8201	23.3204	26.4911	34.0681	34.4101	34.4594	47.016	47.046	3
	seg2	10	0.783582	3.16891	7.39626	14.8214	23.3199	26.4915	34.0675	34.4189	34.462	47.0009	47.0464	3

Continued Table A.2

Description (Class)	segment	Case no.	freq 1	freq 2	freq 3	freq 4	freq 5	freq 6	freq 7	freq 8	freq 9	freq 10	freq 11	Damage index
Horizontal crack	seg2	1	0.778139	3.16472	7.38929	14.7997	23.3098	26.4488	33.8882	34.4493	46.7392	47.0073	54.3354	4
	seg2	2	0.777928	3.16392	7.3863	14.7986	23.3062	26.4436	33.8682	34.4357	46.7873	47.0042	54.2996	4
	seg2	3	0.777956	3.16422	7.38599	14.801	23.3093	26.4476	33.8855	34.4325	46.8553	47.0175	54.2848	4
	seg2	4	0.777974	3.16454	7.3847	14.8051	23.3091	26.4481	33.9127	34.4353	46.7502	47.0272	54.2367	4
	seg2	5	0.777978	3.16263	7.38426	14.8006	23.296	26.3492	33.9425	34.4342	46.7946	47.0033	53.9477	4
	seg2	6	0.777999	3.16477	7.3839	14.8091	23.3036	26.4504	33.9109	34.4468	46.7978	47.0197	54.1939	4
	seg2	7	0.77869	3.16969	7.3919	14.8296	23.3278	26.4293	33.9208	34.4923	46.9539	47.1086	53.9754	4
	seg2	8	0.780719	3.17979	7.41319	14.8612	23.3836	26.4967	33.9171	34.5735	47.0116	47.2234	54.2623	4
	seg2	9	0.780732	3.1799	7.4126	14.8624	23.3804	26.5009	33.9321	34.5786	46.878	47.2194	54.2676	4
	seg2	10	0.780751	3.1799	7.41213	14.8631	23.3783	26.4971	33.9385	34.5826	46.7675	47.2171	54.2524	4
Vertical crack	seg3	1	0.765116	3.20434	7.60296	15.0974	23.9376	26.3889	33.6007	35.1345	48.0749	54.6173	63.3148	5
	seg3	2	0.764931	3.20361	7.60207	15.0973	23.9375	26.3878	33.5971	35.1372	48.0766	54.6137	63.3063	5
	seg3	3	0.764932	3.20347	7.60165	15.098	23.9364	26.3883	33.5971	35.1343	48.0828	54.617	63.3076	5
	seg3	4	0.764897	3.20362	7.60224	15.0992	23.9375	26.3879	33.5961	35.1337	48.0812	54.6192	63.3132	5
	seg3	5	0.764863	3.20283	7.60024	15.0976	23.9369	26.3884	33.5963	35.1306	48.0719	54.6176	63.3065	5
	seg3	6	0.76675	3.2045	7.59485	15.0977	23.9018	26.3538	33.6359	35.0974	48.0099	54.5128	63.1681	5
	seg3	7	0.765298	3.19946	7.58756	15.0831	23.8876	26.3433	33.6059	35.0912	48.0012	54.5006	63.1638	5
	seg3	8	0.764978	3.20337	7.60052	15.0969	23.9357	26.3892	33.5983	35.1321	48.0779	54.6266	63.3083	5
	seg3	9	0.765092	3.20415	7.60172	15.0967	23.9351	26.39	33.6001	35.1304	48.0757	54.6353	63.3116	5
	seg3	10	0.765047	3.20352	7.60102	15.0988	23.9389	26.3901	33.6001	35.1353	48.0805	54.6268	63.3106	5
Horizontal crack	seg3	1	0.766736	3.21002	7.60821	15.1046	23.938	26.4091	33.6074	34.9839	35.1338	47.8689	48.0624	6
	seg3	2	0.766563	3.20873	7.60578	15.0988	23.9305	26.4099	33.6048	34.8943	35.1228	47.9645	48.0413	6
	seg3	3	0.765112	3.20762	7.6113	15.0979	23.9417	26.4012	33.5766	34.8708	35.1364	47.688	48.0603	6
	seg3	4	0.765256	3.2079	7.61225	15.0979	23.9408	26.4047	33.5874	35.0326	35.1361	47.7002	48.0623	6
	seg3	5	0.765348	3.20834	7.61332	15.0996	23.9444	26.4055	33.592	35.0048	35.1372	47.9159	48.0632	6
	seg3	6	0.763987	3.20427	7.60979	15.0918	23.9197	26.4017	33.565	34.8512	35.1004	47.7803	48.0045	6
	seg3	7	0.764408	3.20459	7.60911	15.0963	23.9345	26.406	33.5773	34.7732	35.1184	47.4733	48.0198	6
	seg3	8	0.764823	3.20553	7.60919	15.097	23.9419	26.4065	33.5878	34.8602	35.1334	47.47	48.0477	6
	seg3	9	0.765885	3.20948	7.61392	15.1026	23.9495	26.4114	33.6103	34.9947	35.1442	47.7944	48.0769	6
	seg3	10	0.766167	3.21105	7.61701	15.1086	23.9568	26.413	33.6153	35.0304	35.1503	47.8966	48.082	6

Table A.3. Frequency results for tower with 45 m height

Description (Class)	segment	Case no.	freq 1	freq 2	freq 3	freq 4	freq 5	freq 6	freq 7	freq 8	freq 9	freq 10	freq 11	Damage index
Healthy	–	–	0.469524	2.16104	5.21818	10.092	16.1139	23.3584	26.7099	32.0487	33.6122	42.7416	54.7737	0
Vertical crack	seg1	1	0.429099	1.86917	4.48613	8.66296	13.7052	20.0151	23.7367	27.4006	28.9622	36.3641	46.8139	1
	seg1	2	0.429361	1.86919	4.48639	8.66352	13.705	20.0177	23.7466	27.4035	28.9794	36.3657	46.8153	1
	seg1	3	0.429054	1.86937	4.48555	8.66224	13.7054	20.0196	23.7366	27.4071	28.9707	36.3531	46.7733	1
	seg1	4	0.429526	1.86925	4.48433	8.66112	13.7041	20.0212	23.7637	27.4103	29.017	36.3498	46.7407	1
	seg1	5	0.429642	1.86882	4.48407	8.66153	13.7038	20.0194	23.7628	27.4083	29.0185	36.3485	46.7532	1
	seg1	6	0.429422	1.86897	4.48578	8.66427	13.7081	20.0221	23.7491	27.409	28.9922	36.3571	46.7794	1
	seg1	7	0.428602	1.86995	4.48761	8.66484	13.7084	20.0168	23.7165	27.4005	28.9312	36.3645	46.7995	1
	seg1	8	0.429068	1.8691	4.48704	8.66667	13.7085	20.0218	23.7374	27.4094	28.9732	36.3573	46.7964	1
	seg1	9	0.428859	1.86959	4.4869	8.66465	13.7077	20.0208	23.7316	27.4068	28.9603	36.3538	46.7785	1
	seg1	10	0.428885	1.86993	4.48673	8.66366	13.7067	20.0167	23.7322	27.4017	28.9589	36.3542	46.7681	1
Horizontal crack	seg1	1	0.428837	1.86929	4.48503	8.66002	13.7064	20.0098	23.7316	27.3854	28.9394	36.3519	46.8269	2
	seg1	2	0.42839	1.86941	4.48709	8.66498	13.7075	20.0113	23.7193	27.3822	28.9275	36.3574	46.8236	2
	seg1	3	0.4289	1.8691	4.48422	8.66106	13.7033	20.0113	23.7389	27.3852	28.952	36.3625	46.8156	2
	seg1	4	0.428869	1.86924	4.48596	8.66411	13.7061	20.0166	23.7363	27.3882	28.9457	36.3654	46.8181	2
	seg1	5	0.428811	1.86918	4.48629	8.66458	13.7045	20.0083	23.7383	27.3834	28.9494	36.3513	46.8162	2
	seg1	6	0.428897	1.86917	4.48713	8.66472	13.7049	20.0099	23.7379	27.3882	28.9496	36.3644	46.8164	2
	seg1	7	0.428817	1.86927	4.48721	8.66356	13.7036	20.0082	23.74	27.386	28.9508	36.3632	46.815	2
	seg1	8	0.428724	1.86941	4.48506	8.66031	13.7057	20.0121	23.724	27.3881	28.9275	36.3535	46.8327	2
	seg1	9	0.428276	1.86975	4.48573	8.66148	13.7086	20.0112	23.7036	27.375	28.8979	36.3462	46.835	2
	seg1	10	0.428321	1.86971	4.48481	8.65911	13.7064	20.0038	23.7081	27.3588	28.9009	36.3501	46.8189	2
Vertical crack	seg2	1	0.391727	1.81341	4.35925	8.45322	13.4925	19.5572	22.2006	26.8776	27.9761	35.7157	45.8722	3
	seg2	2	0.391744	1.81336	4.35967	8.45229	13.4927	19.5566	22.2016	26.8762	27.9772	35.718	45.8745	3
	seg2	3	0.391738	1.81326	4.35946	8.45095	13.492	19.5542	22.2009	26.8751	27.9755	35.7162	45.8774	3
	seg2	4	0.391717	1.81308	4.35945	8.45072	13.4926	19.5538	22.1997	26.8754	27.974	35.7133	45.876	3
	seg2	5	0.391727	1.81345	4.35931	8.45311	13.4917	19.5569	22.201	26.8766	27.9764	35.7141	45.8691	3
	seg2	6	0.391837	1.81331	4.35979	8.45093	13.4928	19.5547	22.2041	26.8771	27.9817	35.7192	45.8811	3
	seg2	7	0.391784	1.81331	4.3599	8.45245	13.4935	19.5571	22.2035	26.8785	27.9799	35.7184	45.8751	3
	seg2	8	0.391707	1.81379	4.36011	8.45274	13.4951	19.5568	22.2005	26.8808	27.975	35.7135	45.8752	3
	seg2	9	0.391648	1.81454	4.36006	8.45168	13.4938	19.5564	22.199	26.8748	27.9715	35.7228	45.8742	3
	seg2	10	0.391961	1.8147	4.36062	8.45077	13.4951	19.5607	22.207	26.8823	27.9853	35.7622	45.9078	3

Continued Table A.3

Description (Class)	segment	Case no.	freq 1	freq 2	freq 3	freq 4	freq 5	freq 6	freq 7	freq 8	freq 9	freq 10	freq 11	Damage index
Horizontal crack	seg2	1	0.391656	1.81321	4.35858	8.45181	13.4934	19.5526	22.201	26.8154	27.9702	35.7166	45.8573	4
	seg2	2	0.391611	1.81309	4.35855	8.45143	13.4913	19.5515	22.1995	26.8203	27.9673	35.6875	45.8627	4
	seg2	3	0.391617	1.81277	4.35879	8.45212	13.4919	19.5539	22.1998	26.8114	27.9678	35.6779	45.8754	4
	seg2	4	0.391731	1.81258	4.35789	8.4495	13.4876	19.5533	22.2017	26.8073	27.9704	35.7164	45.874	4
	seg2	5	0.391572	1.81583	4.3618	8.44431	13.4989	19.5458	22.2017	26.815	27.9666	35.7266	45.8549	4
	seg2	6	0.391543	1.81533	4.36215	8.44065	13.5004	19.5369	22.1999	26.8172	27.9631	35.7157	45.8502	4
	seg2	7	0.391708	1.81137	4.35997	8.44919	13.4942	19.5517	22.201	26.8188	27.9709	35.694	45.8765	4
	seg2	8	0.391705	1.81113	4.35895	8.44869	13.49	19.5522	22.2006	26.808	27.9703	35.7189	45.8606	4
	seg2	9	0.391687	1.81152	4.35895	8.44427	13.4924	19.5455	22.2	26.7938	27.9687	35.7047	45.8589	4
	seg2	10	0.391608	1.81294	4.35949	8.44653	13.4981	19.5457	22.2024	26.8054	27.9686	35.6936	45.8685	4
Vertical crack	seg3	1	0.390332	1.80249	4.34661	8.42266	13.4366	19.4554	22.1882	26.7935	27.9956	35.6398	45.7514	5
	seg3	2	0.389596	1.79854	4.33833	8.40961	13.4213	19.4442	22.1834	26.7799	27.9726	35.6305	45.7448	5
	seg3	3	0.390793	1.8047	4.35099	8.42944	13.445	19.4625	22.192	26.8042	28.0107	35.6478	45.7595	5
	seg3	4	0.389522	1.79817	4.33765	8.40886	13.4209	19.4438	22.1831	26.7788	27.9701	35.6304	45.7462	5
	seg3	5	0.390353	1.80248	4.34648	8.42304	13.438	19.4561	22.1888	26.7915	27.9965	35.6361	45.748	5
	seg3	6	0.390601	1.80338	4.34582	8.41153	13.4187	19.4369	22.1909	26.7776	28.0047	35.6283	45.7256	5
	seg3	7	0.390734	1.80427	4.34977	8.42683	13.4409	19.4582	22.1919	26.7955	28.0091	35.6389	45.7503	5
	seg3	8	0.390063	1.80085	4.343	8.41774	13.4327	19.4546	22.1868	26.7962	27.9877	35.6452	45.7581	5
	seg3	9	0.390641	1.80375	4.34864	8.42486	13.4376	19.4529	22.1913	26.7834	28.0063	35.6279	45.7381	5
	seg3	10	0.390444	1.80338	4.3487	8.42581	13.4405	19.4591	22.1895	26.7994	27.9983	35.6442	45.7548	5
Horizontal crack	seg3	1	0.390607	1.80355	4.34639	8.42552	13.4277	19.4429	22.1906	26.7958	28.0028	35.6117	45.7327	6
	seg3	2	0.39051	1.8039	4.34737	8.4258	13.4383	19.4419	22.1895	26.7886	27.997	35.6335	45.73	6
	seg3	3	0.390552	1.8031	4.34483	8.41588	13.4353	19.4398	22.1905	26.7615	28.0017	35.6281	45.7365	6
	seg3	4	0.390587	1.80328	4.34507	8.41231	13.4313	19.4505	22.1907	26.761	28.0031	35.6084	45.7354	6
	seg3	5	0.390568	1.80308	4.34463	8.41005	13.4225	19.4502	22.1911	26.7781	28.0033	35.608	45.718	6
	seg3	6	0.390607	1.80351	4.34647	8.41353	13.4223	19.4409	22.1909	26.7855	28.0047	35.6364	45.7343	6
	seg3	7	0.390594	1.80386	4.34863	8.41961	13.428	19.4374	22.1907	26.7721	28.0038	35.6272	45.7503	6
	seg3	8	0.390404	1.80236	4.34497	8.41568	13.4218	19.4326	22.1895	26.7592	27.9989	35.6106	45.7267	6
	seg3	9	0.390525	1.80302	4.34687	8.42149	13.4325	19.4471	22.1905	26.7718	28.0029	35.6173	45.7266	6
	seg3	10	0.390762	1.80445	4.35021	8.4277	13.4422	19.4593	22.1922	26.7977	28.0099	35.6409	45.7518	6